INFLUENCE OF ANISOTROPIC SCATTERING ALONG THE 2D-FERMI SURFACE ON TRANSPORT PROPERTIES IN AN ASYMMETRIC-DONOR-BASED MOLECULAR CRYSTAL

NATHANAEL A. FORTUNE*†, K. MURATA*, G.C. PAPAVASSILIOU**, D.J. LAGOUVARDOS** AND J. S. ZAMBOUNIS***
*Physical Science Division, Electrotechnical Laboratory, 1-1-4 Umezono, Tsukuba 305 JAPAN
**Theoretical and Physical Chemistry Institute,National Hellenic Research Foundation, 48, Vassileos Constantinou Avenue, Athens 116/35 Greece
***Materials Research Laboratory, CIBA-GEIGY AG, 1723 Marly 1, Switzerland
†Internet: fortune@etlrips.etl.go.jp

ABSTRACT

We report our results for the temperature dependence of the Hall coefficient and in-plane resistivity for the asymmetric-donor-based quasi-2D molecular crystal τ-(P-*S*,*S*-DMEDT-TTF)$_2$ $(AuBr_2)_1(AuBr_2)_y$ (y ≈ 0.75). Using a recent "geometrical representation" of the weak-field 2D Hall conductivity developed by N.P. Ong [Phys. Rev. B **43**, 193 (1991)], we model the temperature dependence of these electronic transport properties in terms of the temperature dependence of the scattering path length and its anisotropy along the 2D Fermi surface.

EXPERIMENT

The charge-transfer salt (P-*S*, *S*-DMEDT-TTF)$_2(AuBr_2)_1(AuBr_2)_y$ has a tetragonal crystal structure with unit cell dimensions a = 7.3546(6) Å and c = 67.977(7) Å and molecules that pack in a τ-type molecular arrangement [1]. Elemental analysis indicates that y ≈ 0.75. The molecular structure of the asymmetric donor is shown in Fig. 1. In the τ-phase structure, the large, planar donors do not stack, but instead arrange themselves edge to edge with the long axis parallel to the c-axis. There are intermolecular S---N and S---S contacts forming a 2D conducting grid parallel to the ab-plane. This salt is expected to be a 2D metal (for y < 1) with a band structure similar to other τ-phase salts such as τ-(EDOVDT-TTF)$_2(I_3)_1(I_3)_y$ [2]. Measurements of the in-plane and out-of-plane conductivity for this [1] and other τ-phase salts [2] are consistent with 2D metallic conductivity in the ab plane and a diverging resistivity out of the plane.

The thinnest platelets were a light, translucent brown, while thicker platelets were an opaque black. Intermediate thickness (10±2 μm and 15±2 μm) black platelets with flat surfaces were selected. Most of the platlets exhibited macroscopic twinning, forming triangle and pyramid patterns visible under an ordinary optical microscope. Triangular shaped regions free of visible twins were cleaved and trimmed so that the long axis ran parallel to the twin boundary edge.

Fig. 1: Molecular structure of the asymmetric donor (P-*S*,*S*-DMEDT-TTF).

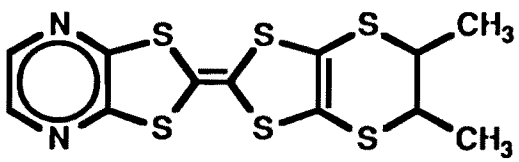

P-*S*,*S*-DMEDT-TTF

Mat. Res. Soc. Symp. Proc. Vol. 328. ©1994 Materials Research Society

Electrical contact to the sample was made by repeatedly evaporating a thin film of Au through a shadow mask onto the sample so that the current contacts at the far ends of the sample wrap around the longitudinal axis of the sample and completely cover the end faces (this helps provide a uniform current distribution). 20 μm Au wires were attached to the Au contacts with Ag paint. For the resistivity sample, voltage contacts also wrap completely around the longitudinal axis. For the Hall sample, the voltage contacts partially wrap around the longitudinal axis, covering the thin side face and part of the top and bottom faces. Two sets of Hall contacts were included on the Hall sample to check for any systematic errors. Both pairs of Hall voltage contacts gave identical results within the scatter of the data. While the longitudinal resistance was also measured for both sets of contacts on the Hall sample, the absolute value of the resistivity for the Hall effect sample is susceptible to systematic errors due to the contact geometry. Sample dependences due to variations in $AuBr_2$ concentration y or crystal defects (microcracks, etc) will also introduce systematic errors. In this experiment, the resistivities scale between the two samples between 10 K and 200 K but the absolute value of the resistivity for the Hall effect sample is approximately three times larger.

The direction of the 5 tesla magnetic field and current were varied to eliminate spurious contributions to the Hall effect from the longitudinal resistance, transverse magnetoresistance and thermoelectric effects; the poorer signal to noise ratio at higher temperatures results from the increasing longitudinal resistance, the decreasing Hall resistance and temperature instabilities.

The temperature dependence of the resistivity for currents in the ab plane (2D plane) is shown (for the resistivity sample) in Fig 2. The resistivity drops to approximately 1/10 of its room temperature value between 100 and 10 K, then begins to increase again with decreasing temperature down to at least 0.7 K. The rise in resistivity below 10 K is not understood, but may be indicative of electron localization or an incipient metal-insulator transition.

The temperature dependence of the Hall coefficient for currents in the 2D conducting plane (ab plane) and magnetic field applied normal to the 2D plane is shown in Fig. 3. The Hall coefficient is small, negative and apparently temperature independent above 200 K, but quickly diverges in magnitude with decreasing temperature down to 10 K. The magnitude of the Hall coefficient at 1.2 K (not shown) is 1/2 of its value at 10 K.

ANALYSIS AND DISCUSSION

The divergence of the Hall coefficient between 10 K and 200 K can not be described by temperature-independent models of the Hall effect such as the free-electron model or band structure calculations that assume an isotropic electron-phonon scattering time. Since only one band crosses the Fermi surface (FS), a two-band model is also inappropriate. Even for a single band, however, the magnitude of the Hall conductivity is known to be sensitive to the local FS curvature [3] and to variations in the electron-phonon scattering time along the Fermi surface [4].

In principle, the unusual temperature dependence of the weak-field Hall coefficient $R_{Hall}(T)$ and resistivity $\rho(T)$ observed here can be described in terms of the curvature of the Fermi surface κ, the Fermi velocity v_k, and the scattering time τ_k at each point $\mathbf{k}$ on the Fermi surface ($\hbar v_k = \partial \varepsilon_k / \partial \mathbf{k}$). We show here that by employing a recently developed geometrical interpretation of the weak-field Hall conductivity in 2D metals [5], we can use measurements of $\rho(T)$ and $R_{Hall}(T)$ to (1) separate the distinct contributions of negative FS curvature, anisotropy in the scattering path length $l(k)$ and the ratio of the FS area to FS circumference and (2) model the temperature dependence of $\rho(T)$ and $R_{Hall}(T)$ in terms of the temperature dependence of the anisotropy in the scattering path length over the FS.

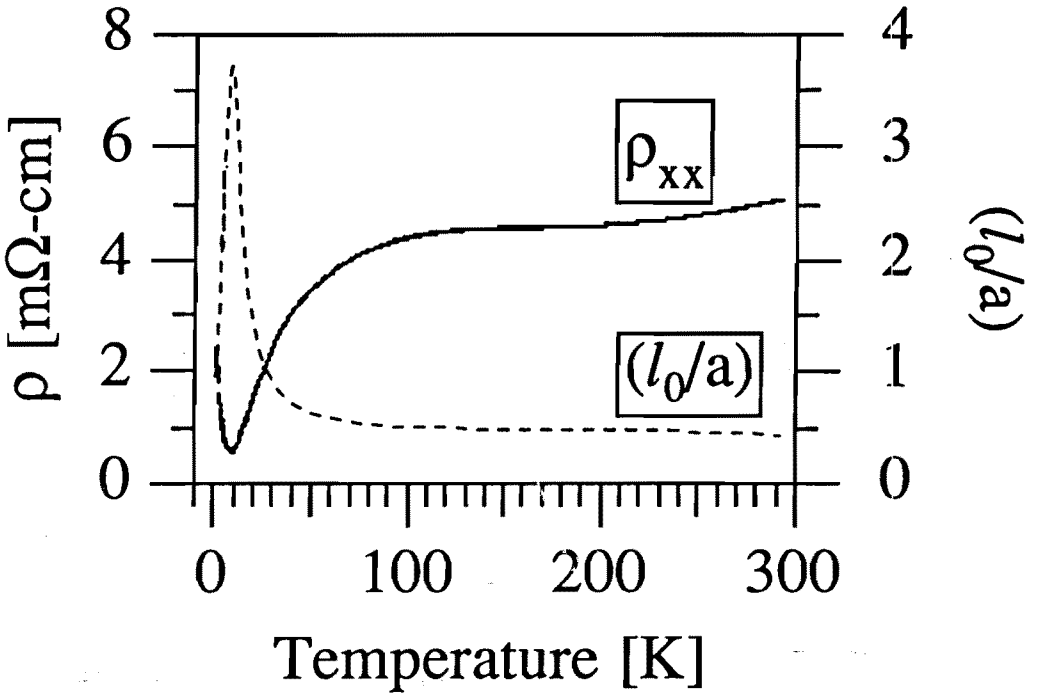

Fig. 2. The temperature dependence of the measured in-plane resistivity ρ_{xx} (left-hand scale) and calculated minimum scattering path length l_0 over the Fermi surface (right-hand scale).

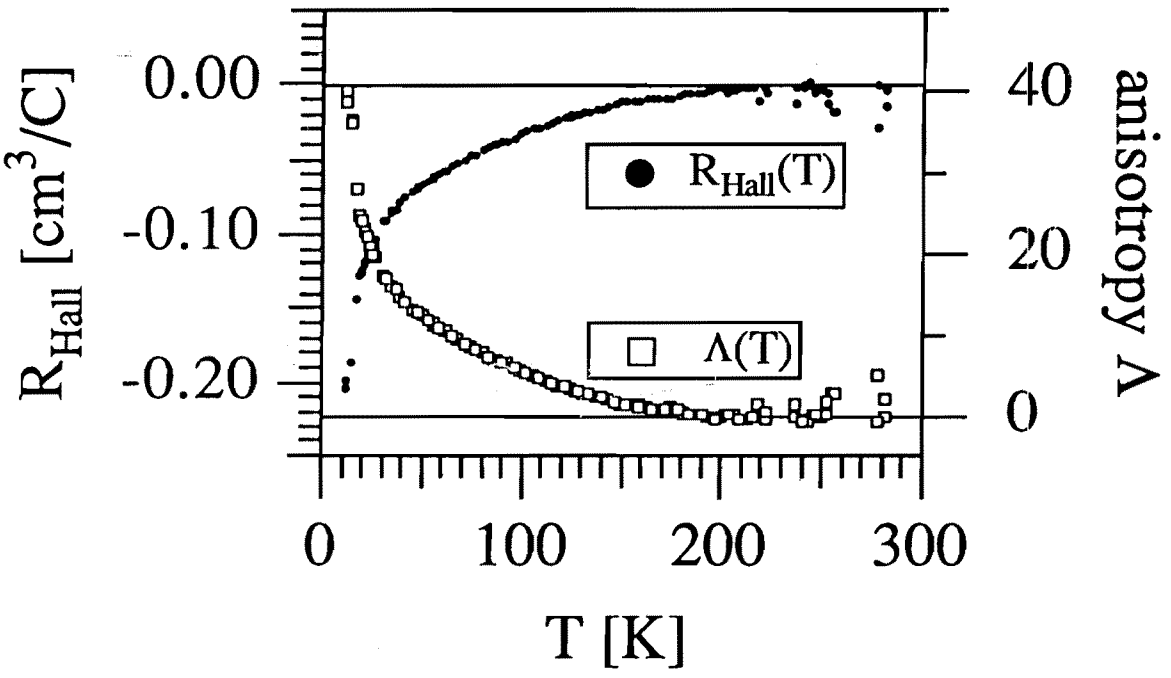

Fig. 3. The temperature dependence of the Hall coefficient R_{Hall}(T) for magnetic field normal to the 2D plane (left-hand side) and the calculated anisotropy Λ in the scattering path l_k over the Fermi surface, where $\Lambda(T) \equiv \sqrt{\pi}\lambda(T) + \frac{\sqrt{\pi}}{8}\lambda^2(T)$ and $\lambda = (l_{max}-l_0)/l_0$ (right-hand side).

To begin, we need to convert the measured longitudinal resistivity $\rho(T)$ and Hall resistivity ρ_{Hall} to the corresponding calculated conductivities (note that the Hall resistivity and Hall coefficient are related by $R_{Hall}(T) = B \bullet \rho_{Hall}(T)$). In general, resistivity ρ and conductivity σ in 3D are nine-element second-rank tensors. If the coupling between in-plane and out-of-plane effects is small enough to be neglected–that is, if an electric field applied normal to the xy plane along the z axis (parallel to the applied magnetic field B) produces a current only along the z axis–then $\sigma_{xz} = \sigma_{zx} = \sigma_{yz} = \sigma_{zy} = 0$. In this case, the relation between element ρ_{ij} and its inverse σ_{ij} can be written [6] as

$$\rho_{xx} = (\sigma_{yy})/\|\sigma\|;\ \rho_{yy} = (\sigma_{xx})/\|\sigma\|;\ \rho_{zz} = 1/\sigma_{zz} \tag{1a}$$

$$\rho_{xy} = -(\sigma_{xy})/\|\sigma\| \tag{1b}$$

$$\|\sigma\| = (\sigma_{xx}\sigma_{yy} - \sigma_{xy}\sigma_{yx}). \tag{1c}$$

If the magnetic field is applied along an axis of greater than 2 fold symmetry, then $\sigma_{XX} = \sigma_{yy}$ and $\sigma_{xy} = -\sigma_{yx}$ (in the 2D weak field limit, $\sigma_{xy} = -\sigma_{yx}$ is always true [5]). In this case, Eqs. (1) for the in-plane longitudinal and Hall resistivities reduce to [6]

$$\rho_{xx} = (\sigma_{xx})/(\sigma_{xx}^2 + \sigma_{xy}^2) \approx 1/\sigma_{xx} \tag{2a}$$

$$\rho_{xy} = -\sigma_{xy}/(\sigma_{xx}^2 + \sigma_{xy}^2) \approx -\sigma_{xy}/\sigma_{xx}^2 \tag{2b}$$

where the second approximate equalities are for ρ_{XX} and ρ_{XY} in the weak-field limit.

For 2D metals in the weak-field, semi-classical limit, Ong [5] has shown that the Hall conductivity σ_{xy}^{2D} has a simple representation in terms of the scattering path length vector $l(\mathbf{k}) = \mathbf{v}_k \tau_k$. Specifically,

$$\sigma_{xy}^{2D} = (e^2/h) A_l/(\pi l_B^2) \tag{3a}$$

$$A_l = (\mathrm{B}/B) \cdot \tfrac{1}{2} \oint_{FS} dl \times l \tag{3b}$$

where the "Stokes area" A_l is the area swept out by the vector $l(\mathbf{k})$ as $\mathbf{k}$ moves around the Fermi surface (FS) and $l_B = \sqrt{\hbar/(eB)}$ is the magnetic length. The temperature-independent anisotropy of $\mathbf{v}_k$ can be determined from band structure calculations, since $\hbar \mathbf{v}_k = \partial \varepsilon_k / \partial \mathbf{k}$. For electron-phonon scattering, τ_k is expected to be isotropic for $T > T_{Debye}$ but become anisotropic for $T < T_{Debye}$. Hence the anisotropy in the scattering path length vector $l(\mathbf{k})$ is T dependent.

Since τ-(P-*S*,*S*-DMEDT-TTF)$_2$(AuBr$_2$)$_1$(AuBr$_2$)$_y$ is tetragonal (4 fold symmetric for B||c), $\sigma_{XX} = \sigma_{yy}$. For a single-band FS in the weak-field, semiclassical 2D limit [5],

$$\sigma_{xx}^{2D} = \sigma_{yy}^{2D} = \tfrac{e^2}{h} l_{av} S/(2\pi) \tag{4a}$$

$$l_{av} = \tfrac{1}{S} \oint_{FS} l_k ds \tag{4b}$$

where S is the FS circumference and l_{av} is the average of l_k (l_k= |l(k)|)over the entire FS. Substituting into the weak-field limit of Eq. (2b) and re-expressing in terms of the "Hall factor" r,

$$r = (B/ne)^{-1}\rho_{xy} = \Gamma A_t/(\pi l_{av}^2) \tag{5a}$$

$$\Gamma = 4\pi A_{FS}/S^2 \tag{5b}$$

$$A_{FS} = 2\pi^2 n_{2D} \tag{5c}$$

where Γ is a geometric constant relating the FS area A_{FS} to the FS circumference S and n_{2D} is the 2D carrier density [5]. The Hall factor r is related to the Hall coefficient R_{Hall}(T) by

$$r = \frac{R_{Hall}(T)}{R_{Hall}^{free}}\bigg|_{3D} = \frac{R_{Hall}(T)}{R_{Hall}^{free}}\bigg|_{2D} = \frac{R_{Hall}(T)}{(1/ne)}\bigg|_{2D} \tag{6a}$$

$$n_{3D} = \left(n_{2D}/t_{layer}\right) \tag{6b}$$

where t_{layer} is the thickness of each 2D metallic layer. Here, t_{layer} = c/2.

It remains to (1) calculate n_{2D}, Γ and R_{Hall}^{free} from the (band-structure-derived) FS and (2) calculate l_k and l_{av} from the expected anisotropy of l_k over the FS. For y = 0.75, band structure calculations [2] for the τ-phase salts predict either a small area 4-pointed star FS or a large area distorted square FS with rounded corners. As is discussed in detail elsewhere [5,7], only the distorted square FS is consistent with the high temperature (T>200 K) limit and temperature dependence of R_{Hall}(T). We estimate that $0.785 < \Gamma < 1$ and that the distorted square FS occupies 92% of the first Brillioun zone (BZ) for y = 0.75. This corresponds to a $R_{Hall}^{free}\big|_{3D} = -6.25\times10^{-3}$ cm^3/C (3D), close to the measured value of $R_{Hall}(T)\big|_{T>200K} \approx -5\times10^{-3}$cm^3/C. If we assume that TDebye ≈ 200 K, then -5 x 10^{-3} cm^3/C corresponds to the temperature-independent isotropic τ limit [5]for R_{Hall}(T).

As the temperature decreases, scattering becomes more intense on the low curvature 'flat' sides than at the high curvature corners of the distorted square FS [4, 5, 8] . Because of the proximity of the flat sides to the BZ boundary and transformation of the FS shape from distorted square FS to 4-pointed star FS for a small increase in energy (small decrease in y), the magnitude of v_k is larger at the FS corners than on the sides. This 'anomalous' variation in v_k along the FS gives rise to an anisotropic scattering path length l_k that is longer at the corners than on the sides of the FS. Most importantly, the anisotropy in l_k *increases* as T decreases. If we assume a Gaussian variation in l_k with $l_k = l_0$ on the FS sides and reaching a maximum $l_k = l_0 + \Delta l = l_{max}$ at the corners, then

$$l_{av}(T) = l_0\left(1 + \tfrac{\pi^{1.5}}{8}\eta\lambda(T)\right) \approx l_0 \tag{7a}$$

$$\lambda \equiv (l_{max} - l_0)/l_0 \tag{7b}$$

where η<<1 and λ is a measure of the anisotropy of l_k over the FS [5, 7].

We can calculate ρ_{3D} by substituting Eq. (7a) into Eq. (4a) to find σ_{xx}^{2D}, inverting according to Eq. (2a) to find ρ_{xx}^{2D}, then scaling by the layer thickness. Similarly, by using Eqs. (3a) and (3b) to find σ_{xy}^{2D}, substituting σ_{xx}^{2D} and σ_{xy}^{2D} into Eq. (2b) to find ρ_{xy}^{2D}. Finally, scaling by the layer

thickness we can calculate r and $R_{Hall}(T)|_{3D}$. The results are [5, 7]

$$\rho_{xx}(T)\big|_{3D} = (h/4e^2)t_{layer}[a/l_{av}(T)] \approx (h/4e^2)t_{layer}[a/l_0(T)] \tag{8a}$$

$$R_{Hall}(T)\big|_{3D} = R_{Hall}^{free}\big|_{3D}\Gamma(l_0/l_{av})^2[1+\Lambda(T)] \approx R_{Hall}^{free}\big|_{3D}\Gamma[1+\Lambda(T)] \tag{8b}$$

$$\Lambda(T) \equiv \sqrt{\pi}\lambda(T) + \tfrac{\sqrt{\pi}}{8}\lambda^2(T). \tag{8c}$$

Thus $\rho_{xx}(T)$ is a measure of the (temperature-dependent) minimum scattering path length over the FS while $R_{Hall}(T)$ is a measure of the anisotropy in the scattering path length over the FS. *$R_{Hall}(T)$ will be temperature dependent if the degree of anisotropy $\lambda(T)$ is temperature dependent, even for a single band.* For $T>T_{Debye}$, where the electron-phonon scattering time τ_k becomes isotropic ($\tau_k = \tau_0$), $\lambda(T)$ becomes temperature independent. Thus in the high T limit, $R_{Hall}(T)$ becomes temperature independent, as expected from isotropic τ_k models.

In this model, the 'anomalous' divergence of $R_{Hall}(T)$ between 10 K and 200 K simply reflects the unusual variation of the scattering path length over the FS. The calculated temperature variation of $l_0(T)$ and $\lambda(T)$ is plotted using the right hand scales in Fig. 2 and Fig. 3, respectively. This variation is a consequence of the (band-structure-derived) anisotropy in v_k and the standard (temperature-dependent) anisotropy in the electron-phonon scattering time τ_k over the FS. In the range of temperatures, pressures and magnetic field for which quasi-2D molecular conductors such as τ-(P-*S*,*S*-DMEDT-TTF)$_2$(AuBr$_2$)$_1$(AuBr$_2$)$_y$ can be considered multilayer 2D metals, this analysis provides an understanding of the temperature-dependence of the weak-field Hall coefficient. Measurements of $\rho_{xx}(T)$ and $R_{Hall}(T)$, in tandem with high-field magnetoquantum oscillation measurements and band-structure calculations, can now act as powerful probes of the FS in these materials. Conversely, measurements of $\rho_{xx}(T)$ and $R_{Hall}(T)$ can now be used as an additional test of the accuracy of band-structure calculations.

REFERENCES

1. J.S. Zambounis, J. Pfeiffer, W. Hofherr, G. Rihs, A. Terzis, P. Delhaes, G.C. Papavassiliou (unpublished).

2. G. C. Papavassiliou, D.J. Lagouvardos, V.C. Kakoussis, A. Terzis, A. Hountas, B. Hilti, C. Mayer, J.S. Zambounis, J. Pfeiffer, M-H. Whangbo, J. Ren and D.B. Kang (Mater. Res. Soc. Proc. 247, 1992) pp. 535-540.

3. M.Tsuji, J. Phys. Soc. Jpn. **13**, 979 (1958).

4. J.M. Ziman, Phys. Rev. **121**, 1320 (1961).

5. N.P. Ong, Phys. Rev. B **43**, 193 (1991).

6. A.B. Pippard, Magnetoresistance in Metals (Cambridge University Press, Cambridge,1989).

7. N.A. Fortune, K. Murata, G.C. Papavassiliou, D.J. Lagouvardos And J. S. Zambounis (unpublished).

8. J.M. Ziman, Electrons and Phonons (Clarendon, Oxford, 1960).